FACTA UNIVERSITATIS
Series: **Electronics and Energetics** Vol. 34, Nº 1, March 2021, pp. 89-104
https://doi.org/10.2298/FUEE2101089P

Original scientific paper

GPU-SUPPORTED SIMULATION FOR ABEP AND QOS ANALYSIS OF A COMBINED MACRO DIVERSITY SYSTEM IN A GAMMA-SHADOWED K-μ FADING CHANNEL

Nenad Petrović[1], Selena Vasić[2], Dejan Milić[1], Suad Suljović[1], Samir Koničanin[1]

[1]Faculty of Electronic Engineering, University of Niš, Serbia
[2]Faculty of Information Technologies, Metropolitan University, Belgrade, Serbia

Abstract. *In this paper we have analyzed macro-diversity (MD) system with one macro SC diversity (MD SC) receiver and two micro MRC (mD MRC) receivers over correlated Gamma-shadowed k-μ fading channel. The average bit error probability (ABEP) is calculated using the moment generating function (MGF) approach for BDPSK and BPSK modulations. Graphical representation of the results illustrates the effects of different parameters of the system on its performance as well as the improvements due to the benefits of a combined micro and macro diversity. The obtained analytical expressions are used for the GPU-enabled mobile network modeling, planning and simulation environment to determine the value of Quality of Service (QoS) parameter. Finally, linear optimization is proposed as an approach to improve the QoS parameter of the fading-affected system observed in this paper.*

Key words: *Gamma shadowing, k-μ fading, MGF, ABEP, GPGPU, SDR*

1. INTRODUCTION

In cellular communications, due to specific nature of transmission channels, signal power level at the receiver is affected by macroscopic and microscopic degrading effects [1]. Macroscopic effects are usually shadowed fading effects from buildings, foliage, and other objects. Microscopic fading is a result of multipath characteristics. In urban areas, there is no direct line-of-sight (LoS) along the transmission line. The channel characteristics between transmitter and receiver will change instantaneously as the mobile user moves in the environment with not-stationary surrounding objects that additionally affect the transmission. Therefore, a multipath fading, a shadowed fading, or a mixture of these two can characterize

Received July 22, 2020; received in revised form November 4, 2020
Corresponding author: Nenad Petrović
Faculty of Electronic Engineering, University of Niš, Aleksandra Medvedeva 14, 18000 Niš, Serbia
E-mail: nenad.petrovic@elfak.ni.ac.rs

© 2021 by University of Niš, Serbia | Creative Commons License: CC BY-NC-ND

the transmission channel [2]. In overcrowded downtown environments where foliage and urban shadowing is found, both multipath and shadowed fading need to be considered while analyzing system performances. Long-scale fading is manifested in variations of the signal average strength at the receiver. Small-scale fading emerges in the form of rapid fluctuations of the amplitude and phase of a signal. In a homogeneous channel short-term fading is successfully described by Rayleigh, Nakagami-*m*, Rice or Hoyt distributions. In a real system, the surfaces are spatially correlated, so the channel is non-homogeneous [3]. Distributions that model non-homogeneous fading channels are generalized *n*-distribution and generalized *q*-distribution. They are valid in both cases-when LoS (line-of-sight) component is present or absent and are more appropriate in modeling practical fading channels. Parameterized distributions such as κ-μ and η-μ distributions are used to model this type of non-homogeneous channels which show functional similarities with generalized-*n* and generalized-*q* distributions, respectively. The η-μ distribution is used to model the non-homogeneous small-scale fading in the absence of LoS component [4]. Distribution κ-μ is generalized distribution used to model small-scale fading in line-of-sight (LoS) non-homogeneous fading channel. For μ=1, κ-μ distribution becomes Rice distribution, for $\kappa \to 0$ Nakagami-*m* distribution, for μ=1, $\kappa \to 0$ Rayleigh distribution, and for μ=0.5, $\kappa \to 0$ one-sided Gaussian distribution [5]. Applying diversity techniques eliminates negative effects of fading [6].

Diversity combining improves receiver performance by processing numerically statistically independent copies of the same signal carrying information across multiple fading channels and by efficiently combining the two or more signals. The idea behind this concept is that it is highly unlikely that deep fading will simultaneously occur in all the diversity channels, thus reducing error probability. The minimum antenna spacing for a mobile unit is at least half a wavelength [7]. Macro-diversity (MD) reception reduces both long-term and short-term fading effects on performance of cellular mobile radio systems [8]. MD reduces the shadowing effect, and micro-diversity (mD) systems decrease rapid fading. MRC and EGC combining techniques, followed by SC and SSC techniques reduce the impact of fading and increase channel capacity [9]. MRC and EGC combiners are complex to implement in practice; hence, the use of SC combining, especially in cases with minimal correlation between channels, has proved as more efficient. The SC receiver choses the branch with the highest signal-to-noise ratio (SNR). For MRC harvesters, if the noise power is equal at all inputs the square of the output signal is equal to the sum of the squares of the input signals [10].

In this paper, a combined MD system with MD SC receiver and two mD MRC receivers in a Gamma-shadowed k-μ multipath fading channel is analyzed. Using the calculated expression for the moment-generating function (MGF) of the signals at the output of the mD MRC receivers, MGF of the signal at the output of MD SC receiver is determined. In the following, the obtained expression for MGF can be used to evaluate the first-order statistics such as outage probability (OP) and bit error probability (BEP) of the observed MD system. The average bit error probability (ABEP) for non-coherent binary differential phase-shift keying (BDPSK) and non-coherent binary phase-shift keying (BPSK) is studied using the MGF-based approach. To the best authors' knowledge deriving ABEP using MGF method for the combined MD system with MD SC receiver and two mD MRC receivers in a Gamma large-scale fading and κ-μ small-scale fading in a simulated

environment is not analyzed in open technical literature. Numerical results are obtained using software Mathematica and Origin and they illustrate the proposed analytical expressions and impact of the parameters of the system on the statistical characteristics observed. Moreover, the derived expressions were integrated in GPU-enabled mobile network modeling, planning and simulation environment.

The paper is organized in the following way: In Section II, system ABEP is calculated for BFSK and BDPSK modulations schemes of the observed system using MGF approach. In Section III, numerical results and the corresponding analysis of the system performance are presented. GPU-enabled modelling, simulation and network planning environment for the system undergoing conditions described in this paper are given in Section IV. The conclusion is presented in Section V.

2. Average Bit Error Probability over Moment Generating Function

In this section macro diversity system (MD) with MD SC receiver and two mD MRC receivers in a channel affected by Gamma long-term and k-μ short-term fading is investigated. The block-diagram of a macro-diversity model under consideration is shown in Fig. 1. The envelopes of the useful signals at the inputs of the first and the second L-branch mD are denoted by: $r_{11,}\ldots,r_{1L}$, where $r_{21,}\ldots,r_{2L}$ are the second mD inputs, and x_1 and x_2, as the outputs of mDs. The envelope of the useful signal at the output of MD SC receiver is denoted by r.

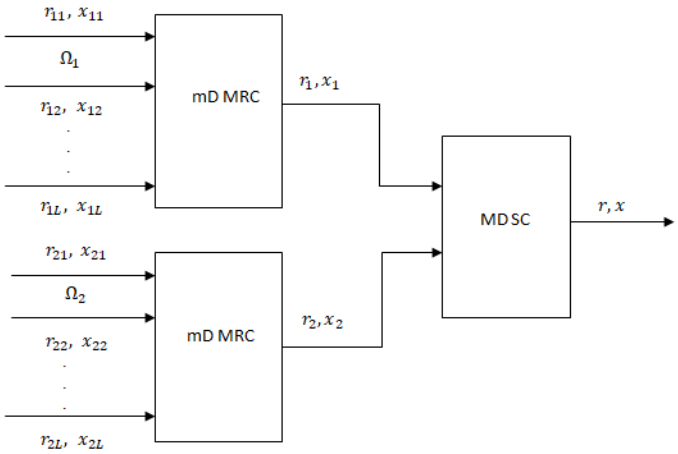

Fig. 1 Block-diagram of the combined MD system

In mobile radio channels with LoS (Line-of-Sight) components the envelopes of the useful signals $r_{ij,}$ affected by a small-scale fading, follow the κ-μ distribution [11]:

$$p_{r_{ij}}(r_{ij}) = \frac{2\mu r_{ij}^{\mu}}{e^{\mu K} K_i^{\frac{\mu-1}{2}}} \left(\frac{K_i+1}{\Omega_i}\right)^{\frac{\mu+1}{2}} e^{-\frac{\mu(K_i+1)}{\Omega_i} r_{ij}^2} I_{\mu-1}\left(2\mu r_{ij}\sqrt{\frac{K_i(K_i+1)}{\Omega_i}}\right) \quad (1)$$

In the above expression $I_0(x)$ denotes modified Bessel function of the first kind and of zeroth order, $\Omega_i = \overline{x_{ij}^2}$ are the powers of the useful signals, $x_{ij} \geq 0$. Parameter μ describes the number of multipath clusters. The smaller values of μ cause the increase in fading severity. The parameter K describes the ratio of the power of a dominant component and the power of the scattered components.

In the considered environment with a dominant *LoS* component, after the transformation $x_{ij}=r_{ij}^2$, $x_{ij}\geq 0$; $i=1,2$, $j=1,2..L.$, the PDF of k-μ random variable x_i can be written as [12]:

$$p_{x_i}(x_i|\Omega_i) = \frac{L\mu_i}{e^{L\mu_i K_i}}\left(\frac{K_i+1}{L\Omega_i}\right)^{\frac{L\mu_i+1}{2}}\left(\frac{x_i}{K_i}\right)^{\frac{L\mu_i-1}{2}} e^{-\frac{\mu_i(K_i+1)}{\Omega_i}x_i} I_{L\mu_i-1}\left(2L\mu_i\sqrt{\frac{K_i(K_i+1)x_i}{L\Omega_i}}\right) \quad (2)$$

Using well-known transformation [13; 17.7.1.1] the modified Bessel function of the first kind can be written as:

$$I_v(x) = \sum_{k=0}^{\infty}\frac{x^{v+2k}}{2^{v+2k}\,k!\,\Gamma(v+k+1)}. \quad (3)$$

where $\Gamma(m)$ is the Gamma function. Using the expression (3) we can obtain the PDF of the SNR at the output of the mD MRC combiner:

$$p_{x_i}(x_i|\Omega_i) = e^{-\frac{\mu_i(K_i+1)}{\Omega_i}x_i - L\mu_i K_i}\sum_{i=0}^{\infty}\frac{(LK_i)^i\,\mu^{2i+L\mu}\,x_i^{\,i+L\mu-1}}{i!\,\Gamma(i+L\mu_i)}\left(\frac{K_i+1}{\Omega_i}\right)^{i+L\mu_i} \quad (4)$$

Parameter μ can take only integer values as it represents the argument in the Gamma function. Moreover, the moment-generating function (MGF) of a random variable $x_{ij} > 0$ is given by [14]:

$$M_{x_i}(s) = \overline{e^{x_i s}} = \int_0^{\infty} dy_{ij}\, e^{-x_i s}\, p_{x_i}(x_i) = \frac{1}{e^{L\mu_i K_i}}\sum_{i=0}^{\infty}\frac{(LK_i)^i\,\mu^{2i+L\mu_{ii}}}{i!}\left(\frac{K_i+1}{\mu_i(K_i+1)+s\Omega_i}\right)^{i+L\mu_i} \quad (5)$$

In the observed system, there are $i=2$ branches of MD SC receiver, and powers of the corresponding useful signals are represented by the random variables Ω_1 and Ω_2. In Gamma-shadowed channels, these random variables follow the correlated Gamma distribution [15], [16]:

$$p_{\Omega_1\Omega_2}(\Omega_1,\Omega_2) = \frac{e^{-(\Omega_1+\Omega_2)/(\Omega_0(1-\rho))}}{\Gamma(c)}\sum_{i=0}^{\infty}\frac{\rho^i(\Omega_1\Omega_2)^{i+c-1}}{i!\,\Gamma(i+c)\Omega_0^{\,2i+2c}(1-\rho)^{2i+c}}. \quad (6)$$

In the last expression, c is the order of the Gamma distribution, Ω_0 denotes the average value of the signal powers Ω_1 and Ω_2 ($\Omega_0 = \overline{\Omega_1} = \overline{\Omega_2}$) and ρ is the correlation coefficient. MD SC receiver selects the signal from the micro diversity MRC receiver that has the largest average power of the signal envelope. Hence, the moment generating function of the signal at the output of the macro diversity SC receiver will be given by [17], [18]:

$$M_x(s) = \int_0^{\infty} \mathrm{d}\Omega_1 \int_0^{\Omega_1} \mathrm{d}\Omega_2 M_{x_1}(s) p_{\Omega_1\Omega 2}(\Omega_1\Omega_2) +$$

$$+ \int_0^{\infty} \mathrm{d}\Omega_2 \int_0^{\Omega_2} \mathrm{d}\Omega_1 M_{x_2}(s) p_{\Omega_1\Omega 2}(\Omega_1\Omega_2) =$$

$$= 2\int_0^{\infty} \mathrm{d}\Omega_1 \int_0^{\Omega_1} \mathrm{d}\Omega_2 M_{x_1}(s) p_{\Omega_1\Omega 2}(\Omega_1\Omega_2). \tag{7}$$

By substituting expressions (5) and (6) in the expression (7), we obtain the MGF at the output of the MD SC receiver:

$$M_x(s) = \frac{2}{\Gamma(c)\mathrm{e}^{L\mu_i K_i}} \sum_{i_1=0}^{\infty}\sum_{i_2=0}^{\infty} \frac{\rho^{i_1}(LK_i)^{i_2}\,\mu_i{}^{2i_2+L\mu_i}(K_i+1)^{i_2+L\mu_i}}{i_1!i_2!\Gamma(i_1+c)\Omega_0{}^{2i_1+2c}(1-\rho)^{2i_1+c}} \cdot$$

$$\cdot \int_0^{\infty} \mathrm{d}\Omega_1 \frac{\Omega_1{}^{i_1+c-1}\mathrm{e}^{-\Omega_1/\Omega_0(1-\rho)}}{(\mu_i(K_i+1)+s\Omega_i)^{i_2+L\mu_i}} \int_0^{\Omega_1} \mathrm{d}\Omega_2 \mathrm{e}^{-\Omega_2/\Omega_0(1-\rho)}\Omega_2{}^{i_1+c-1} \tag{8}$$

The integral I_1 in the above expression is equal:

$$I_1 = \int_0^{\Omega_1} \mathrm{d}\Omega_2 \Omega_2{}^{i_1+c-1}\mathrm{e}^{-\Omega_2/(\Omega_0(1-\rho))} = (\Omega_0(1-\rho))^{i_1+c}\,\gamma\left(i_1+c, \frac{\Omega_1}{\Omega_0(1-\rho)}\right). \tag{9}$$

Here, $\gamma(\alpha, x)$ is lower incomplete gamma function [19; 6.5.2], that can be developed by using the following form of the series [20]:

$$\gamma(\alpha, x) = \frac{1}{a}x^a\mathrm{e}^{-x}\sum_{j=0}^{\infty}\frac{x^j}{(1+\alpha)_j}. \tag{10}$$

where $(a)_n$ denotes the Pochhammer symbol. Using (10), we can evaluate the integral I_1 as follows:

$$I_1 = \frac{\mathrm{e}^{-\Omega_1/(\Omega_0(1-\rho))}}{i_1+c}\sum_{i_3=0}^{\infty}\frac{\Omega_1{}^{i_1+i_3+c}}{(i_1+c+1)_{i_3}(\Omega_0(1-\rho))^{i_3}} \tag{11}$$

After substituting back, the expression (11) into the expression (8) for the MGF at the output of the MD SC receiver, we can rewrite the expression for the MGF as:

$$M_x(s) = \frac{2}{\Gamma(c)\mathrm{e}^{L\mu_i K_i}} \sum_{i_1=0}^{\infty}\sum_{i_2=0}^{\infty}\sum_{i_3=0}^{\infty} \frac{\rho^{i_1}(L\mu_i K_i)^{i_2}}{i_1!i_2!\Gamma(i_1+c)(i_1+c)(i_1+c+1)_{i_3}} \cdot$$

$$\cdot \frac{1}{\Omega_0{}^{2i_1+i_3+2c}(1-\rho)^{2i_1+i_3+c}} \int_0^{\infty} \mathrm{d}\Omega_1 \frac{\Omega_1{}^{2i_1+i_3+2c-1}\mathrm{e}^{-2\Omega_1/\Omega_0(1-\rho)}}{(1+s/(\mu_i(K_i+1))\Omega_i)^{i_2+L\mu_i}} \tag{12}$$

Using the following identity [21; 3.383]:

$$\int_0^\infty \frac{x^{q-1}\mathrm{e}^{-px}}{(1+ax)^v}\mathrm{d}x = a^{-q}\Gamma(q)\Psi\left(q, q+1-v, \frac{p}{a}\right) \tag{13}$$

where ψ (s, d, t) denotes the confluent hyper-geometric function, the last part of the expression (12) labeled as integral I_2, can take the form:

$$I_2 = \int_0^\infty \mathrm{d}\Omega_1 \frac{\Omega_1^{2i_1+i_3+2c-1}\mathrm{e}^{-2\Omega_1/\Omega_0(1-\rho)}}{(1+s/(\mu_i(K_i+1))\Omega_i)^{i_2+L\mu_i}} = \left(\frac{\mu_i(K_i+1)}{s}\right)^{2i_1+i_3+2c} \cdot$$

$$\cdot\Gamma(2i_1+i_3+2c)\Psi\left(2i_1+i_3+2c, 2i_1+i_3+2c+1-i_2-L\mu_i, \frac{2\mu_i(K_i+1)}{\Omega_0 s(1-\rho)}\right) \tag{14}$$

Substituting back the expression for the integral I_2 into expression (12), we obtain the MGF at the output of the MD SC receiver:

$$M_x(s) = \frac{2}{\Gamma(c)\mathrm{e}^{L\mu_i K_i}} \sum_{i_1=0}^\infty \sum_{i_2=0}^\infty \sum_{i_3=0}^\infty \frac{\rho^{i_1}(LK_i)^{i_2}\mu_i^{2i_1+i_2+i_3+2c}}{i_1!i_2!\Gamma(i_1+c)\Omega_0^{2i_1+i_3+2c}} \cdot$$

$$\cdot\frac{\Gamma(2i_1+i_3+2c)}{(1-\rho)^{2i_1+i_3+c}(i_1+c)(i_1+c+1)_{i_3}}\left(\frac{K_i+1}{s}\right)^{2i_1+i_3+2c} \cdot$$

$$\cdot\Psi\left(2i_1+i_3+2c, 2i_1+i_3+2c+1-i_2-L\mu_i, \frac{2\mu_i(K_i+1)}{\Omega_0 s(1-\rho)}\right) \tag{15}$$

One of the performance measures of the wireless communication system is the average symbol error probability (ASEP). If there are two bits per symbol, this property is equivalent to the average bit error probability (ABEP) [8].

In the following, using the obtained expression for MGF, the ABEP of non-coherent BFSK and BDPSK modulation signals can be directly calculated as [6]:

$$\begin{aligned} \mathrm{P}_{\mathrm{be}}(\Omega_0) &= 0.5\mathrm{M}_x(0.5), \text{ for BFSK;} \\ \mathrm{P}_{\mathrm{be}}(\Omega_0) &= 0.5\mathrm{M}_x(1), \text{ for BDPSK.} \end{aligned} \tag{16}$$

Graphical representation of the ABEP for the range of different values of parameters from expression (16) for BFSK and BDPSK modulation is given in Figures 2, 3, 4 and 5.

3. NUMERICAL AND GRAPHICAL RESULTS

Figures 2 and 3 show the ABEP of the MD SC receiver output in terms of the parameter Ω_0 (the average value of the signal powers Ω_1 and Ω_2) for several different values of fading-severity parameters, correlation coefficient ρ and different number of branches (L) on the input of mD MRC receivers for BFSK modulation.

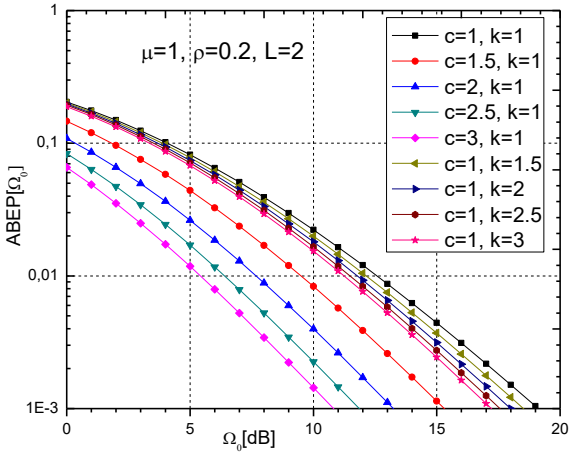

Fig. 2 ABEP in terms of Ω_0 for BFSK modulation and different values of c and K

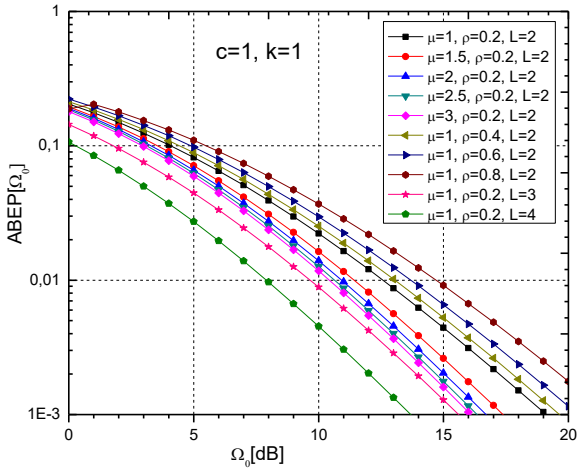

Fig. 3 ABEP in terms of Ω_0 for BFSK modulation and different values of μ, ρ and L

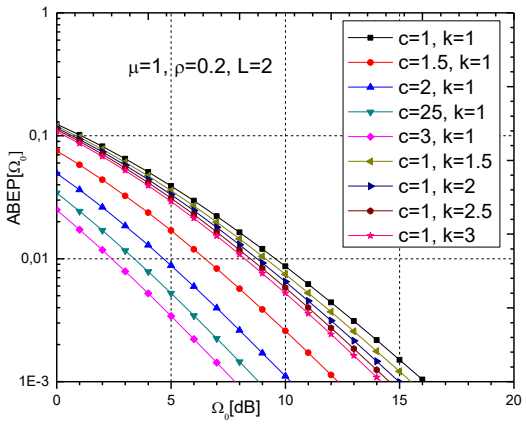

Fig. 4 ABEP in terms of Ω_0 for BDPSK modulation and different values of c and K

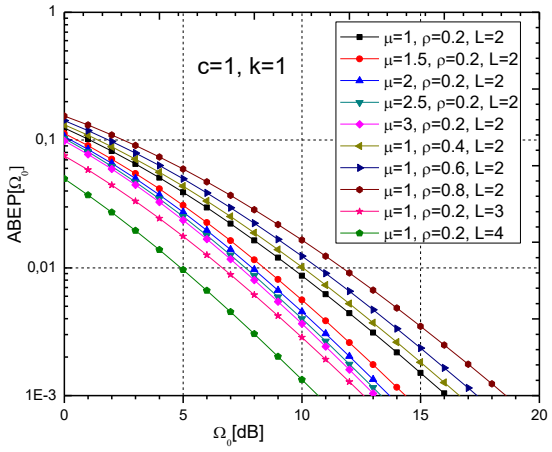

Fig. 5 ABEP in terms of Ω_0 for BDPSK modulation and different values of μ, ρ and L

The figures 2, 3, 4, 5 for both BFSK and BDPSK modulations show that, as parameters μ, c, k and L are increasing ABEP function is decreasing and the system has better performance and stability. The increase in correlation coefficient ρ influences the increase in ABEP and the system becomes unstable. It can be observed that the higher values of Ω_0 lead to a lower error and better performance.

ABEP is significantly reduced with increasing L-input in micro MRC, and the system performance will improve. On the other hand, larger ABEP results in a degradation of system performance. Comparing the graphics results we can conclude that the better stability of the system and a smaller ABEP are achieved for the BDPSK than BFSK modulation.

To further analyze the ABEP performances, error related to truncation of infinite series will be considered.

Tables 1 and 2 illustrate the number of terms in the series that need to be added in order to assure the accuracy of the expression (16) to 5 decimal places, for the given values of BFSK parameters, as given in Figures 2 and 3.

Table 1 Number of terms needed in the infinite series expansion in the expression (16) for the ABEP for the BFSK with accuracy to 5 decimal places: μ=1, L=2, ρ=0.2, while changing parameters c and K (Fig.2).

	Ω_0=0 dB	Ω_0=5 dB	Ω_0=10 dB
c=1, K=1	11	10	7
c=1.5, K=1	12	9	7
c=2, K=1	13	11	7
c=2.5, K=1	13	10	7
c=3, K=1	14	11	8
c=1, K=1.5	13	11	9
c=1, K=2	13	12	11
c=1, K= 2.5	15	14	12
c =1, K=3	18	15	13

For three different values of Ω_0 [dB] and different values of parameters c and K, more terms are needed in the expansion and convergence will occur at a slower pace.

Table 2 Number of terms needed in the infinite series expansion in the expression (16) for the ABEP for the BFSK with accuracy to 5 decimal places, where c=K=1 and parameters μ, ρ and L are varied (Fig.3).

	Ω_0=0 dB	Ω_0=5 dB	Ω_0=10 dB
μ=1, ρ=0.2, L=2	11	10	7
μ=1.5, ρ=0.2, L=2	12	11	10
μ=2, ρ=0.2, L=2	14	13	10
μ=2.5, ρ=0.2, L=2	15	14	13
μ=3, ρ=0.2, L=2	18	15	13
μ=1, ρ=0.4, L=2	13	10	8
μ=1, ρ=0.6, L=2	15	13	10
μ=1, ρ=0.8, L=2	11	20	16
μ=1, ρ=0.2, L=3	11	10	8
μ=1, ρ=0.2, L=4	13	11	10

As the values of the parameters μ, ρ and L increase, the number of terms in the expression needed for the accuracy to 5 decimal places increases too, and convergence is obtained at a slower pace.

In Tables 3 and 4 the results for the similar analysis are presented for the BDPSK modulation scheme. The number of terms in the series expansion in the expression (16) needed to achieve the accuracy to 5 decimal places for the given parameter values, are presented all together with the results given in Figures 4 and 5.

Table 3 Number of terms in the infinite series expansion of the expression (16) for the ABEP for BDPSK at the accuracy of 5 decimal places, where μ=1, L=2, ρ=0.2, and various values of parameters *c* and *K* (Fig.4).

	Ω_0=0 dB	Ω_0=5 dB	Ω_0=10 dB
c=1, *K*=1	11	8	7
c=1.5, *K*=1	11	8	5
c=2, *K*=1	12	9	5
c=2.5, *K*=1	12	9	5
c=3, *K*=1	12	9	5
c=1, *K*=1.5	12	9	8
c=1, *K*=2	13	12	10
c=1, *K*=2.5	14	13	12
c=1, *K*=3	17	15	13

Again, for three different values of the average power Ω_0 [dB] as the parameters *c* and *K* increase, the number of terms needed for the series convergence increases, so convergence is slower.

Table 4 Number of terms in the infinite series expansion of the expression (16) for the ABEP for BDPSK at the accuracy of 5 decimal places, where *c=K=1* and parameters μ, ρ and *L* take various values (Fig.3).

	Ω_0=0 dB	Ω_0=5 dB	Ω_0=10 dB
μ=1, ρ=0.2, L=2	11	8	7
μ=1.5, ρ=0.2, L=2	12	9	9
μ=2, ρ=0.2, L=2	13	11	10
μ=2.5, ρ=0.2, L=2	14	13	12
μ=3, ρ=0.2, L=2	17	15	12
μ=1, ρ=0.4, L=2	12	9	7
μ=1, ρ=0.6, L=2	13	11	7
μ=1, ρ=0.8, L=2	23	17	12
μ=1, ρ=0.2, L=3	10	9	7
μ=1, ρ=0.2, L=4	11	10	9

Table 4 shows that for higher values of the parameters μ, ρ and *L*, more terms should be added in the expression to achieve the accuracy up to and including the fifth decimal, so convergence becomes slower. Also, the higher values of the correlation coefficient require more terms.

4. GPU-ENABLED MODELLING, SIMULATION AND NETWORK PLANNING ENVIRONMENT

4.1. Framework overview

Although many of the network simulators conceptualize mobile propagation models up to some point, often they involve time-consuming and inefficient computational schemes resulting in difference between simulated and realistic scenarios. To assure better simulation results and optimal computation algorithms, in this section, we present the framework for simulated transmission in a gamma-shadowed kappa-mu fading environment analyzed in

the previous sections. The idea behind the efficiency of the approach is the implementation of the GPGPU computational units [22], [23]. The software framework has several phases. In the first phase, user defines mobile network within the graphical environment running in a web browser. Various modelling aspects related to infrastructure, terrain, channel, and service consumers within smart cities, have been considered earlier [24], [25]. The Quality of Service (QoS) parameter values are calculated with the reference to the ABEP values. These values and the user-defined model are taken as the input of a linear optimization mechanism. The process of linear optimization is executed, giving the optimal base station configuration and deployment as output, which is further translated to target Software Defined Radio (SDR) commands. Fig. 6 depicts the modeling and simulation environment used for network planning.

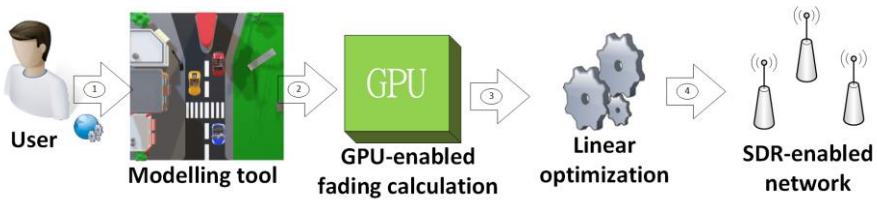

Fig. 6 Overview of GPU-enabled mobile network modeling, planning and simulation environment: 1-Creation of user-defined smart city mobile network model diagram 2-Mobile network model 3-Calculated QoS values 4-SDR commands

4.2. GPU-enabled fading calculation

Traditionally, graphics processing units (GPU) perform computations only for computer graphics. The goal is to implement general-purpose GPU (GPGPU) programming to accelerate the calculations in applications that are not graphic. In [22] and [23], GPGPU has been considered as an effective approach towards performance improvement when it comes to simulations of fading effect. A pseudo-code depicting the structure of CUDA kernel is given in Fig. 7.

```
__global__ void calc_impact(Location* l, float* qi)
{
    int k = threadIdx.x + blockIdx.x * blockDim.x;
    while (k < N)
    {
        qi[k] = MGF(l->o[k])/qnf;
        k += blockDim.x * gridDim.x;
    }
}
```

Fig. 7 GPU-powered CUDA kernel pseudo-code for QoS impact calculation

In this paper, we adopt NVIDIA CUDA for GPU-enabled calculation of ABEP that is further used for QoS estimation of the observed system. The pseudo-code shows how calculations are distributed among different GPU computation/processing subunits to

achieve the speed-up. The input of this algorithm is a set of locations (denoted as *l*) within the map, while the output is a set of QoS impact coefficients determined for each location (denoted as *qi*). To each location, Ω_0 value is assigned (denoted as o) and used as input of MGF function (denoted as *MGF*) to calculate the value of ABEP. Furthermore, *qnf* is used for normalization of ABEP to a real number from range [0, 1] in order to express the weight of fading effect expressed by ABEP value among different parameters that might affect quality of service, as discussed in [25]. This value can be set by user and is determined empirically. Moreover, the obtained result is further used for calculation of the next QoS value at the time point $t+1$ at location L:

$$QoS(\mathrm{t}+1,\ \mathrm{L}) = QoS(\mathrm{t}) \cdot qi(t+1,\ L) \tag{17}$$

To assure the computational pace, Intel i7 7700-HQ quad-core CPU machine at 2.8 GHz and GTX 1050 GPU with 2 GB VRAM, 1TB HDD and 16GB DDR4 RAM is used. According to the results, the GPU-enabled calculation of QoS based on ABEP for this type of fading is around 42 times faster than calculation done on CPU using the tool from [24]. Moreover, the performance improvement using the GPGPU approach for level-crossing rate (LCR) of the SC receiver output over α-κ-μ multipath fading channels [25] was 39 times faster while performance evaluation of MD wireless communication system within Weibull multipath fading channel [26] was 47 times faster.

4.3. Linear optimization and QoS

One of the main objectives in designing and implementing wireless networks is to provide the best possible quality of service (QoS). In this section, we overview the linear optimization approach to improve the QoS in a real-life scenario of the transmission over Gamma long-term and k-μ short-term fading channel employing a combined MD system with MD SC receiver and two mD MRC receivers. In every fading-affected environment, QoS requirements can be recognized in terms of data rates, average bit error rates, delay limits, outage probabilities and so forth. The linear optimization method presented in the following is aimed to assure the best possible data rates and lowest error rates, as well as minimum possible outage probability of the system proposed in the previous sections. The analysis is based on a mathematical model with the requirements expressed by linear relationships [27].

We define the base station $BaseStation_b$, energy consumption ec_b and an estimated capacity, that is the highest number of connected users c_b. Also, we define the location $Location_l$ for each base station and encounter the cost of energy distribution dc_l as well as an estimated demand d_l of service by the customers for the given location covered by the allocated base station. We will contemplate a level of QoS drop *qd[b,l]* for each pair *($BaseStation_b$, $Location_l$)*. This parameter depends not only on the specific characteristics of the channel (in our scenario these would be specific fading conditions) but also the design and properties of the base station itself. The parameter is represented by the ratio between the values of maximum possible and estimated QoS for the observed part of the channel:

$$qd[b,l] = \frac{Q_0 S_{\max}[b,l]}{Q_0 S_{estimate}[b,l]} \tag{18}$$

where *x[b,l]* represents the decision variable. It can take only two possible values: 1 if $BaseStation_b$ is at the $Location_l$, while it takes 0 in the other case. Linear optimization allows for allocating the base stations to optimal locations. This will have positive effects on the QoS parameters such as the minimization of QoS drop, together with reduction of costs related to energy distribution and consumption:

$$minimize \sum_{b \in BaseStation,\ l \in Location} qd[b,l]dc[b,l]ec[b]x[b,l] \tag{19}$$

There are several conditions that must be fulfilled to successfully complete the optimization. Primarily, a single base station has to be assigned to each location:

$$\sum_{b \in BaseStation} x[b,l] = 1,\ l \in Location \tag{20}$$

Moreover, each base station is assigned to at most one location at the moment:

$$\sum_{l \in Location} x[b,l] \leq 1,\ b \in BaseStation \tag{21}$$

Each base station assigned to a specific location has to assure the needed capacity to meet the service demand for the corresponding location:

$$\sum_{b \in BaseStation} c[b]x[b,l] \geq d[l], l \in Location \tag{22}$$

To implement the linear optimization program we have used the AMPL[1] optimization supporting system while the optimization process itself has been completed using IBM CPLEX[2] optimizer and its option of simplex method-based solver.

In Table 5, an overview of the results obtained in optimization for different model sizes is given. The first model represents the number of different configurations of the involved base stations (*nBS*). The second column is the number of considered locations (*nL*). These two values determine the size of the model. The third column represents the time needed for optimization processes for the given model size.

In the last column, a percentage of the cost reduction obtained in each scenario is given. According to the results in the Table 5, we can observe that the cost reduction depends on the specific instance model while the time spent on optimization increases with the increase of the model size.

Table 5 Results of the optimization for different sizes of the network model

Number of base stations [nBS]	Number of locations [nL]	Optimization [s]	Cost reduction [%]
5	4	0.05	77
10	6	0.08	54
15	8	0.14	83

[1] https://ampl.com/

[2] https://www.ibm.com/analytics/cplex-optimizer

5. CONCLUSION

We have considered the combined MD system with one macro-diversity SC receiver and two micro-diversity MRC receivers in a Gamma long-term and κ-μ short-term fading channel has been studied. Micro-diversity combines signal envelopes from multiple L antennas at the base stations. In this way multiple effects of κ-μ fading are reduced. On the other hand, MD combines signals with antennas at two or more base stations which helps mitigating the effects of a long-term fading. We have derived the closed-form expressions for the moment-generating function of the signal at the output of the system for correlated composite non-homogenous fading channel for two modulation schemes: BFSK and BDPSK.

Using the obtained expressions, analytical expressions for ABEP for both modulation schemes are evaluated. The ABEP is improved with an increase of the number of antennas L. The increase in correlation coefficient ρ weakens the system performance. The correlation coefficient ρ has higher influence on ABEP for higher values of Gamma long-term fading severity parameters. When ρ is one, the lowest value of the signal occurs simultaneously resulting in MD-reception becoming mD-reception.

The ABEP function is smaller and the system performance is better when the number of branches in mD is greater than L=2. In order to estimate the rate at which the convergence of the expressions for ABEP developed in the infinite series occurs, the analysis has been conducted where the needed number of terms of the series is determined for the rounding accuracy of 5 decimal places. It is observed that the series converges at a high rate, and in general, 10-15 terms need to be taken to achieve the expected accuracy. The increase of the values of parameters μ, ρ and L affects the convergence rate as more terms should be encountered to assure the stated accuracy.

In the final section of the work, we have proposed the implementation of GPU-powered calculations that significantly speed up the determination of QoS parameters based on ABEP function. This is of the utmost importance for the QoS performances in real-time wireless systems dealing with data transmission such as real-time video. The usage of GPGPU in a simulated model of a Gamma long-term and κ-μ short-term fading environment dramatically improves the response. Within the analysis for the improvement in QoS parameter of the fading-affected system observed in this paper the linear optimization is proposed.

The idea behind the linear optimization model is built on the optimal base station configuration and deployment scheme that can be further translated to target Software Defined Radio (SDR) commands. The implementation of command generation mechanisms for specific SDR hardware solutions is outside the scope of this paper and will be covered by our future research. Moreover, we would like to include the channel capacity calculation techniques [28] to dynamically determine the capacity parameter in linear optimization model.

Acknowledgement: *This paper has been supported by the Ministry of Education, Science and Technological Development of the Republic of Serbia.*

REFERENCES

[1] T. S. Rappaport, *Wireless Communications Principles and Practice*. Prentice Hall, 2007.

[2] P. S. Bithas, N. C. Sagias, and P. T. Mathiopoulos, "The bivariate generalized-KKG distribution and its application to diversity receivers", *IEEE Trans. on Commun.*, vol. 57, no. 9, pp. 2655–2662, Sep. 2009.

[3] P. Bithas, N. Sagias, and T. Tsiftsis, "Performance analysis of dual-diversity receivers over correlated generalised Gamma fading channels", *IET Commun.*, vol. 2, no. 1, pp. 174–178, 2008.

[4] R. Subadar, T. S. B. Reddy and P. R. Sahu, "Performance of an L-SC Receiver over kappa-mu and eta-mu Fading Channels", In Proceedings of the IEEE International Conference on Communications, Cape Town, 2010, pp. 1-5.

[5] M. D. Yacoub, "The κ−μ distribution: A general fading distribution", In Proceedings of the IEEE Atlantic City Fall Vehicular Technology Conf., October 2001, pp. 1427–1432.

[6] M. K. Simon and M. S. Alouni, *Digital Communication Over Fading Channels*. 2nd Ed., New Jersey: Wiley-Interscience; 2005.

[7] G. L. Stuber, *Principles of Mobile Communications.* 2nd Ed. Norwell MA: Kluwer Academic Publishers, 2001.

[8] A. S Lioumpas, A. P Doukeli and G. K Karagiannidis, "Another look at multibranch switched diversity systems", *IEEE Commun. Lett.*, vol. 11, no. 4, pp. 325-327, 2007.

[9] P. G. Stavrianos, P. S. Bithas and D. S. Kalivas, "An analytical study for an efficient multi-branch switched diversity receiver", *Int. J. Commun. Syst.*, vol. 30, 2017.

[10] E. A. Neasmith and N. C. Beaulieu, "New Results in selection diversity", *IEEE Trans. Commun.*, vol. 46, no. 5, pp. 695–704, 1998.

[11] M. D. Yacoub, "The κ-μ distribution and the η-μ distribution", *IEEE Antennas Propag. Mag.*, vol. 49, no. 1, pp. 68-81, 2007.

[12] S. R Panić, D. M Stefanović, I. M Petrović, M. Č Stefanović, J. A Anastasov and D. S Krstić, "Second-order statistics of selection macrodiversity system operating over Gamma shadowed κ-μ fading channels", *EURASIP J. Wirel. Commun. Netw.*, no. 151, 2011.

[13] W. Pearson, S. Olver and M. A. Porter, *Numerical methods for the computation of the confluent and Gauss hypergeometric functions*. The Numerical Algorithms Group (NAG) and the Engineering and Physical Sciences Research Council (EPSRC), June 2016.

[14] N. Sekulovic and M. Stefanović, "Performance Analysis of System with micro and macro-diversity Reception in Correlated Gamma Shadowed Rician Fading Channels", *Wirel. Pers. Commun.*, vol. 65, pp 143–156, July 2012.

[15] P. M. Shankar, "Macrodiversity and Microdiversity in Correlated Shadowed Fading Channels", *IEEE Trans. Veh. Technol.*, vol. 58, no. 2, February 2009.

[16] S. Suljović, D. Milić, S. Panić, Č. Stefanović and M. Stefanović, "Level crossing rate of macro diversity reception in composite Nakagami-*m* and Gamma fading environment with interference", vol. 102, p. 102758, May 2020.

[17] S. Panic, J. Anastasov, M. Stefanovic, and P. Spalevic, *Fading and Interference Mitigation in Wireless Communications*. CRC Press: USA, 2013.

[18] D. Krstic, S. Vasić, S. Koničanin, S. Suljović and M. Stefanović, "MGF Based Calculation of ABEP for Macrodiversity Receiver over Gamma-Shadowed Fading Environment with Line-of-Sight", In Proceedings of the 5th International Conference on Smart and Sustainable Technologies (SpliTech), 23-26 September 2020, pp. 1-5.

[19] M. Abramowitz and Irene A. Stegun, *Handbook of Mathematical Function with Formulas, Graphs and Mathematical Tables.* National Bureau Applied Mathematics, series 55, December 1972.

[20] S. Suljović, D. Krstić, D. Bandjur, S. Veljković and M. Stefanović, "Level Crossing Rate of Macro-diversity System in the Presence of Fading and Co-channel Interference", *Rev. Roumaine des Sciences Techniques-Série Électrotechnique et Énergétique*, vol. 64, no. 1, pp. 63–68, 2019.

[21] I. Gradshteyn, I. Ryzhik, *Tables of Integrals, Series, and products*. Academic Press, New York 1994.

[22] A. F. Abdelrazek, M. Kaschub, C. Blankenhorn and M. C. Necker, "A Novel Architecture using NVIDIA CUDA to speed up Simulation of Multi-Path Fast Fading Channels", In Proceedings of the VTC Spring 2009 - IEEE 69th Vehicular Technology Conference, Barcelona, Spain, 2009, pp. 1-5.

[23] R. Carrasco-Alvarez, J. V. Castillo, A. C. Atoche and J. O. Aguilar, "A Fading Channel Simulator Implementation Based on GPU Computing Techniques", *Math. Probl. Eng.*, vol. 2015, pp. 1-8, 2015.

[24] N. Petrović, S. Koničanin, D. Milić, S. Suljović and S. Panić, "GPU-enabled Framework for Modelling, Simulation and Planning of Mobile Networks in Smart Cities", In Proceedings of the Zooming Innovation in Consumer Technologies Conference (ZINC), Novi Sad, Serbia, 2020, pp. 280-285.

[25] D. Milić, S. Suljović, N. Petrović, S. Koničanin and S. Panić, "Software environment for performance of relay signal by DF technique influenced by κ-μ fading", In Proccedings of the 19th International Symposium INFOTEH-JAHORINA, East Sarajevo, Bosnia and Herzegovina, 2020, pp. 1-4.

[26] S. Suljović, D. Milić and S. Panić, "LCR of SC Receiver Output Signal over α-κ-μ Multipath Fading Channels", *FU Elec. Energ.*, vol. 29, no. 2, pp. 261-268, 2016.

[27] S. Suljović, D. Milić, Z. Nikolić, S. Panić, M. Stefanović and Đ. Banđur, "Performance of macro diversity wireless communication system operating in Weibull multipath fading environment", *FU Elec. Energ.*, vol. 30, no. 4, pp. 599-609, 2017.

[28] Z. Ji, C. Dong, Y. Wang, and J. Lu, "On the analysis of effective capacity over generalized fading channels", In Proceedings of the IEEE International Conference on Communications (ICC 2014) - Communications Theory, 2014, pp. 1977-1983.